

# Effects of rising temperature on the formation and microbial degradation of marine diatom aggregates

Judith Piontek<sup>1,\*</sup>, Nicole Händel<sup>1</sup>, Gerald Langer<sup>1</sup>, Julia Wohlers<sup>2</sup>, Ulf Riebesell<sup>2</sup>, Anja Engel<sup>1</sup>

<sup>1</sup>Alfred Wegener Institute for Polar and Marine Research, Am Handelshafen 12, 27570 Bremerhaven, Germany

<sup>2</sup>IFM-Geomar, Leibniz Institute of Marine Science, Düsterbrookweg 20, 24105 Kiel, Germany

**ABSTRACT:** Effects of elevated temperature on the formation and subsequent degradation of diatom aggregates were studied in a laboratory experiment with a natural plankton community from the Kiel Fjord (Baltic Sea). Aggregates were derived from diatom blooms that developed in indoor mesocosms at 2.5 and 8.5°C, corresponding to the 1993 to 2002 mean winter *in situ* temperature of the Western Baltic Sea and the projected sea surface temperature during winter in 2100, respectively. Formation and degradation of diatom aggregates at these 2 temperatures in the dark were promoted with roller tanks over a period of 11 d. Comparison of the 2 temperature settings revealed an enhanced aggregation potential of diatom cells at elevated temperature, which was likely induced by an increased concentration of transparent exopolymer particles (TEP). The enhanced aggregation potential led to a significantly higher proportion of particulate organic matter in aggregates at 8.5°C. Moreover, the elevated temperature favoured the growth of bacteria, bacterial biomass production, and the activities of sugar- and protein-degrading extracellular enzymes in aggregates. Stimulating effects of rising temperature on growth and metabolism of the bacterial community resulted in an earlier onset of aggregate degradation and silica dissolution. Remineralization of carbon in aggregates at elevated temperature was partially compensated by the formation of carbon-rich TEP during dark incubation. Hence, our results suggest that increasing temperature will affect both formation and degradation of diatom aggregates. We conclude that the vertical export of organic matter through aggregates may change in the future, depending on the magnitude and vertical depth penetration of warming in the ocean.

**KEY WORDS:** Diatom aggregates · Temperature · Degradation · Extracellular enzymes · Bacterial growth · Global warming

Resale or republication not permitted without written consent of the publisher

## INTRODUCTION

Phytoplankton aggregates are hotspots of bacterial activity in marine systems (Alldredge & Silver 1988, Simon 2002) and comprise a variety of biological and chemical processes on small spatial and temporal scales. The formation of macroscopic phytoplankton aggregates (i.e. marine snow) has frequently been observed during phytoplankton blooms, particularly those dominated by diatoms (Smetacek 1985, Riebesell 1991, Kjørboe et al. 1996). Aggregates are the main vehicles in the export of organic matter from the surface

ocean and drive the sequestration of particulate organic carbon (POC) to the deep sea (Fowler & Knauer 1986, Asper 1987). The efficiency of aggregate export is controlled by a number of factors, of which the rate of aggregate formation, aggregate size, sinking velocity, and bacterial degradation activity are the most important. Aggregation and degradation of organic matter were shown separately to be sensitive to changing temperature. Thornton & Thake (1998) demonstrated that the formation of aggregates from nitrate-limited continuous cultures of *Skeletonema costatum* was positively correlated with temperature. The rate of bacter-

\*Email: judith.piontek@awi.de

ial aggregate degradation depends primarily on growth and metabolic activity of the associated bacterial community and on the quality of aggregated organic matter (Grossart & Plough 2001). Temperature has been proposed as a principally limiting or supporting factor for microbial processes (Pomeroy & Wiebe 2001). Growth of isolated marine bacterial strains, for example, followed the Arrhenius law over a broad range of temperatures (Wiebe et al. 1992, Pomeroy & Wiebe 2001). Cell-specific growth rates in natural bacterial populations more than doubled when temperature was increased experimentally from 10 to 26°C. Moreover, within the same temperature range, the cell-specific respiratory CO<sub>2</sub> production increased by a factor of approximately 4.7 (Jiménez-Mercado et al. 2007). Bacterial growth requires suitable organic substrates, provided by the degradation of organic matter. The initial step in organic matter degradation is the hydrolysis of high molecular weight compounds by bacterial extracellular enzymes (Hoppe et al. 1993, Arnosti 2004). Enzymatically catalyzed reactions are known to show an optimum curve with respect to temperature. Increasing temperatures accelerate enzymatic reactions as long as they do not cause damage or denaturation of proteins. For instance, Rath & Herndl (1994) showed that the activity of β-glucosidase extracted from marine snow increased until a temperature optimum of about 40°C was reached, and decreased strongly at 50°C. In their study, thermostability of β-glucosidase was improved if enzymes were associated with marine snow.

Temperature effects on the cycling of organic matter in the ocean, and the underlying mechanisms, are of interest to better predict consequences of global warming. Since effects of rising temperature on phytoplankton aggregates cannot be estimated by investigating individual processes, we conducted an encompassing experiment that integrated temperature effects on (1) growth and aggregation of phytoplankton cells, and (2) bacterial degradation of aggregates. Winter–spring blooms occurring in the Kiel Fjord (Western Baltic Sea) were used as a suitable model system. For the Baltic Sea region, an increase in winter sea surface temperature of up to 10°C by 2100 is predicted (IPCC 2001). Here, we report temperature effects on the formation, biogeochemical properties, and microbial degradation of aggregates derived from natural diatom communities that were grown at present-day and elevated temperatures (+6°C).

## MATERIALS AND METHODS

**Experimental setup.** The experiment was conducted as part of the AQUASHIFT indoor mesocosm study in

2006 that investigated the impact of temperature changes on the biology and biogeochemistry of phytoplankton blooms. The general setup of the AQUASHIFT mesocosms is described in more detail in Sommer et al. (2007). Briefly, a natural phytoplankton community was collected from the Western Baltic Sea (Kiel Fjord) and incubated in 8 mesocosms in 4 temperature-controlled walk-in rooms. Temperatures of 2.5, 4.5, 6.5 and 8.5°C were applied to duplicate mesocosms with a volume of 1400 l each. Calculated from the decadal mean between 1993 and 2002, 2.5°C was chosen as the *in situ* temperature in the Kiel Fjord during winter and early spring (Sommer et al. 2007). A 12 h light:12 h dark cycle was applied. The light regime simulated the daily course of light intensities based on season-dependent database values derived from a model using astronomic formulae (Brock 1981). The maximum light intensity was 179 μmol photons m<sup>-2</sup> s<sup>-1</sup>. After the addition of 13 μmol l<sup>-1</sup> nitrate, an initial nitrate concentration of 21 μmol l<sup>-1</sup> was achieved in all mesocosms. The initial phosphate concentration was 0.9 μmol l<sup>-1</sup> in all mesocosms. Hence, inorganic nutrients yielded a N:P ratio of 23.3 in all mesocosms, indicating a phosphate deficiency relative to the Redfield ratio (Redfield et al. 1963).

For the purpose of the present study, aggregates were formed experimentally from particulate matter produced in the duplicate mesocosms at 2.5 and 8.5°C. Aggregation and sedimentation of diatoms in the ocean mainly occurs after the peak of blooms (Smetscek 1985, Riebesell 1991, Kiørboe et al. 1996); therefore, material for the aggregation experiment was collected from the mesocosms 4 d after the bloom peak, defined as the maximum concentration of chlorophyll *a* (chl *a*). The peak of the bloom in the mesocosms at 8.5°C occurred 6 d earlier than at 2.5°C (J. Wohlers et al. unpubl. data). The aggregation experiment was therefore conducted with a time shift of 6 d between the 2 temperature treatments.

In order to harvest sinking particulate matter, including phytoplankton cells and detrital material, organic matter that had sedimented from the water column was drawn from the bottom of the mesocosms with a peristaltic pump. For each mesocosm, the collected material was diluted with mesocosm water to obtain similar particle volumes for all incubations. The suspensions were carefully mixed and transferred into roller tanks. Organic matter of duplicate mesocosms per temperature was incubated separately. A series of 5 roller tanks per mesocosm was prepared, thus yielding a total of 20 tanks in 4 incubation series. Mean values and standard deviations presented in the present study are derived from these duplicates per temperature treatment. Each roller tank had a diameter of 23 cm and contained a volume of 5 l. In order to pro-

mote aggregation, all tanks were placed on roller tables and were rotated with 0.5 rpm in the dark at temperatures of 2.5 and 8.5°C, respectively (Fig. 1).

**Sampling.** Sampling of each incubation series was performed at the start of the experiment and after 60, 108, 156, 204, and 252 h. Macroscopic aggregates (>2 mm) and seawater with dispersed particulate organic matter (POM) were sampled separately after removing roller tanks from the roller table and allowing aggregates to settle to the bottom of the tank. All aggregates were then isolated with a serological pipette and pooled into an aggregate slurry. The volume of the aggregate slurry containing all macroscopic aggregates from the roller tank was determined using a 500 ml graduated cylinder. After all aggregates were removed, the surrounding seawater (SSW) was sampled and its volume determined with a 1000 ml graduated cylinder. It was assumed that aggregates comprised only a relatively small fraction of the total slurry volume due to the simultaneous uptake of SSW during manual aggregate isolation. In order to calculate the amounts of particulate components in the aggregate fraction (AGG), amounts in the SSW were subtracted from those in the slurry according to Engel et al. (2002). Hence, the proportions of particle volume (PV), particulate organic carbon (POC), nitrogen (PON), and phosphorous (POP), transparent exopolymer particles (TEP), and chlorophyll *a* (chl *a*) were calculated as follows:

$$\text{AGG} = v(\text{sl})c_x(\text{sl}) - v(\text{sl})c_x(\text{SSW}) \quad (1)$$

where  $v(\text{sl})$  is the slurry volume,  $c_x(\text{sl})$  is the concentration of parameter  $x$  in the slurry and  $c_x(\text{SSW})$  is the concentration of parameter  $x$  in the SSW. PV and amounts of POC, PON, POP, TEP, and chl *a* were normalized to 1 l of tank volume.

**Biogeochemical analyses.** The aggregate slurry and SSW were analyzed separately. In order to produce a homogeneous suspension for subsampling, aggregate slurries were diluted 1:50 with 0.2  $\mu\text{m}$ -filtered and autoclaved seawater and agitated gently. For measurements of POC, PON, and POP, duplicate samples of 20 ml diluted aggregate slurry and 250 ml SSW were filtered onto precombusted GF/F filters (Whatman) and stored at  $-20^\circ\text{C}$  until further processing. Prior to analysis, filters were dried for 12 h at  $80^\circ\text{C}$ . POC and PON were measured on a CHN-analyser (NA-1500, Carlo Erba). For the analysis of POP, samples were digested with peroxy sulphate at  $120^\circ\text{C}$  for 30 min. After digestion, POP was measured as dissolved orthophosphate according to Koroleff (1977).

For the analysis of TEP, triplicate samples of 5 to 10 ml aggregate slurry and 25 ml SSW were filtered onto 0.4  $\mu\text{m}$  polycarbonate filters and stained with Alcian Blue, a cationic copper phthalocyanine dye that complexes carboxyl and half-ester sulphate reactive groups of acidic polysaccharides. Samples were stored

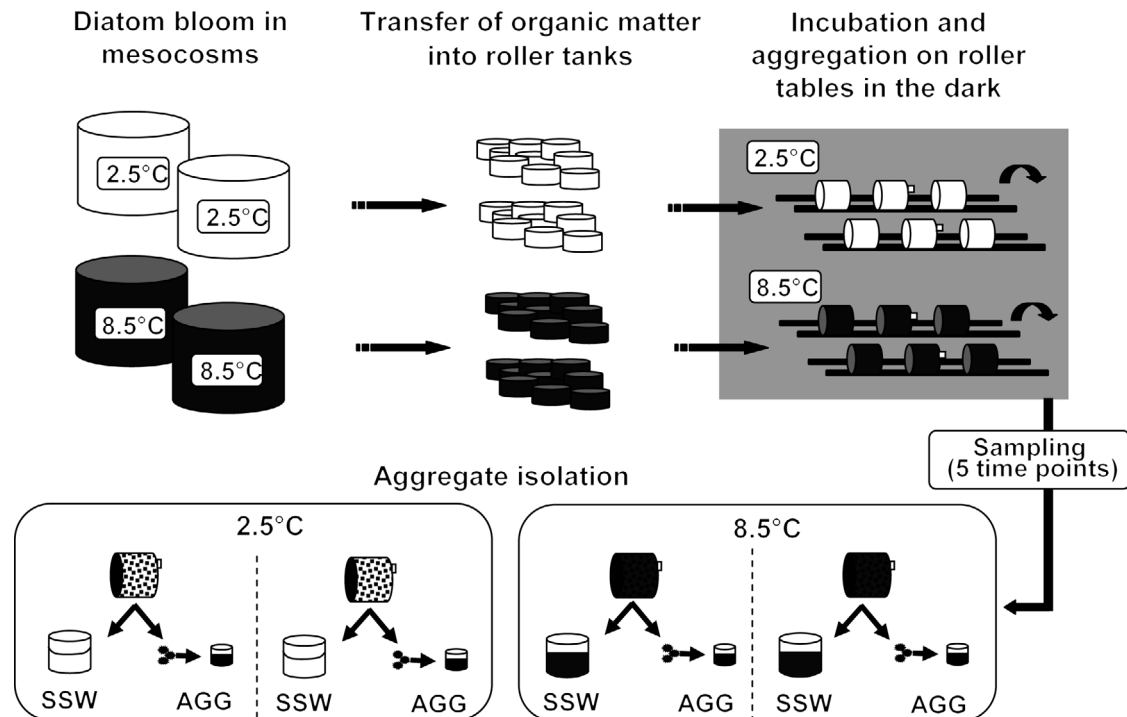


Fig. 1. Experimental setup and sampling design. See 'Materials and methods'. AGG: aggregates; SSW: surrounding seawater

frozen at  $-20^{\circ}\text{C}$  until analysis. TEP concentrations were measured photometrically ( $\lambda = 787 \text{ nm}$ ) and expressed in xanthan equivalents per litre ( $\text{Xeq l}^{-1}$ ) (Passow & Alldredge 1995). A factor of 0.75 was assumed to convert TEP ( $\mu\text{g Xeq}$ ) into carbon units (TEP-C,  $\mu\text{g C}$ ) (Engel & Passow 2001).

Samples for determination of chl *a* were filtered onto GF/F filters (Whatman) and stored at  $-20^{\circ}\text{C}$  in the dark. Prior to analysis, filters were homogenized with an ultrasonic mixer and pigments were extracted with 80% acetone (Strickland & Parsons 1974). Chl *a* concentration was determined with a fluorometer (excitation: 480 nm, emission: 685 nm) and corrected for phaeopigments by measuring the fluorescence before and after acidification of samples with 1 N hydrochloric acid.

A Coulter counter (Multisizer II, Beckman) equipped with a 100  $\mu\text{m}$  aperture, was used to determine PV of aggregates and SSW. The volume of particles between 2.8 and 60  $\mu\text{m}$  equivalent spherical diameter was determined and summed up to yield PV. Prior to analysis, aggregates were broken down so efficiently that all particles were small enough to pass through the aperture and their volume was subsequently detected. This was confirmed by particle size spectra of broken aggregates provided by the Coulter counter measurements, which revealed that more than 90% of the detected particle volume was derived from particles smaller than 40  $\mu\text{m}$ . Analysis was done in triplicate, each with 2 ml of sample.

Dissolved silicate (dSi) was determined in undiluted SSW according to the method of Koroleff (1977) using an autoanalyzer. Ammonium molybdate reacts with dSi in seawater, generating a blue molybdate complex. After reduction with oxalic acid, the dSi concentration can be measured photometrically.

**Microbiological analyses.** All microbiological analyses were performed for aggregate slurries and SSW, respectively. Rates and bacterial cell numbers were normalized to 1 ml of aggregates and SSW, respectively. For enumeration of bacteria, samples were filtered onto black, 0.2  $\mu\text{m}$  pore size polycarbonate filters (Whatman) and stained with 4'6'diamidino-2-phenolindole (DAPI) (Porter & Feig 1980). Samples were stored at  $-20^{\circ}\text{C}$ . Cells were counted using an epifluorescence microscope (Axioplan, Zeiss) at 1000 $\times$  magnification within 4 wk after sampling. At least 1000 cells per sample were counted for statistical evaluation.

Bacterial biomass production (BBP) was determined by incorporation of  $^3\text{H}$ -thymidine (Fuhrman & Azam 1982). Samples of 5 to 10 ml diluted aggregate slurry were incubated in triplicate with a saturating final concentration of 10 nM  $^3\text{H}$ -thymidine. Samples were incubated for 90 min in the dark at 2.5 and  $8.5^{\circ}\text{C}$ . After incubation, samples were poisoned with 2% formalin

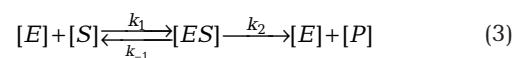
(final concentration) to stop growth and filtered onto 0.2  $\mu\text{m}$  polycarbonate filters (Sartorius). Filters were rinsed with ice-cold 5% trichloroacetic acid and radioassayed by liquid scintillation counting. For calculation of BBP from thymidine incorporation, a conversion factor of  $2 \times 10^{18}$  cells  $\text{mol}^{-1}$  thymidine and a carbon conversion factor of  $0.3 \times 10^{-6}$   $\mu\text{g C } \mu\text{m}^{-3}$  cell were applied (Ducklow & Carlson 1992). A mean cell volume of  $0.03 \mu\text{m}^3 \text{ cell}^{-1}$  was assumed. The cumulative BBP represents the overall BBP during the 252 h of incubation as calculated from the measured rates and the incubation time.

The activity of bacterial extracellular enzymes was measured in the diluted aggregate slurries and the SSW using fluorogenic substrate analogues (Hoppe 1983). The reaction velocities of  $\alpha$ - and  $\beta$ -glucosidase, leucine-aminopeptidase, and alkaline phosphatase were determined by the use of 4-methylumbelliferyl- $\alpha$ -glucopyranoside, 4-methylumbelliferyl- $\beta$ -glucopyranoside, L-leucine-4-methyl-7-coumarinylamide, and 4-methylumbelliferyl-phosphate, respectively. Fluorogenic substrate analogues were added to subsamples of 200  $\mu\text{l}$  volume to final concentrations ranging from 0.2 to 1000  $\mu\text{mol l}^{-1}$ . Samples were incubated in duplicate for 3 h in the dark at 2.5 and  $8.5^{\circ}\text{C}$ . Fluorescence was measured with a microtiter plate fluorometer (Fluoroskan Ascent, Thermo Labsystems; excitation 355 nm, emission 460 nm).

The velocity ( $V$ ) of enzymatic hydrolysis followed Michaelis-Menten kinetics in all samples. Hence, data were fitted according to the equation:

$$V = \frac{V_{\max} [S]}{K_m + [S]} \quad (2)$$

using the software SigmaPlot 9.0. Here,  $S$  is the substrate concentration ( $\mu\text{mol l}^{-1}$ ),  $V_{\max}$  is the maximum velocity of the enzymatic reaction (i.e. the maximum hydrolysis rate) ( $\mu\text{mol l}^{-1} \text{ h}^{-1}$ ), which is attained at saturating substrate concentration, and  $K_m$  ( $\mu\text{mol l}^{-1}$ ) is the Michaelis constant. The Michaelis-Menten kinetic describes the single-substrate mechanism for an enzyme reaction:



where  $E$  is the enzyme,  $ES$  the enzyme-substrate complex,  $P$  the product of the enzymatic reaction, and  $k_1$ ,  $k_{-1}$ ,  $k_2$  the rate constants of the individual steps. As  $V_{\max}$  evaluates the catalytic step of enzymatic substrate degradation at saturating substrate concentration, it is defined by:

$$V_{\max} = k_2 [E] \quad (4)$$

The binding strength between the enzyme and the substrate molecule is given by  $K_m$ , an inverse measure of the enzyme affinity:

$$K_m = \frac{k_{-1} + k_2}{k_1} \quad (5)$$

In order to characterize the enzymatic degradation of a substrate, it is useful to apply a parameter including both the catalytic and the substrate binding step. This is especially reasonable when dealing with a complex natural system that contains unknown concentrations of enzymes and substrates. The ratio  $V_{\max}/K_m$  describes the efficiency of enzymatic substrate degradation as a function of the affinity, catalytic capacity, and concentration of the enzyme:

$$\frac{V_{\max}}{K_m} = \frac{k_1}{k_{-1} + k_2} k_2 [E] \quad (6)$$

The ratio of  $V_{\max}/K_m$  is helpful to assess the enzymatic degradation of substrates at low, non-saturating concentrations.

For comparison of enzymatic activities at 2.5 and 8.5°C, an enhancement factor ( $I$ ) was calculated as follows:

$$I = \frac{x(8.5^\circ\text{C})}{x(2.5^\circ\text{C})} \quad (7)$$

where  $x$  is the mean value over incubation time of  $V_{\max}$ ,  $V_{\max}/K_m$ , and cell-specific  $V_{\max}$ , in aggregates and in SSW at 8.5 and 2.5°C, respectively. All values are presented as means  $\pm$  SD.

## RESULTS

### Bloom development in the mesocosms

In all mesocosms, build-up and decline of phytoplankton blooms dominated by diatoms were observed. After 3 to 7 d, chl *a* started to increase exponentially in the mesocosms at 8.5°C (elevated temperature) and 2.5°C (*in situ* temperature). Algal growth resulted in a drawdown of nitrate and phosphate in all mesocosms. Maximum chl *a* concentration was reached between Days 11 and 19, and was not significantly different between the 2 temperatures. After the peak, chl *a* decreased rapidly and sedimentation of particles to the bottom of the mesocosms was observed. When organic matter was collected from the mesocosms for dark incubations in roller tanks, phosphate and nitrate were depleted in all mesocosms. The stoichiometry of suspended POM at 8.5 and 2.5°C revealed ratios of [PON]:[POP] higher than the Redfield ratio, indicating that algal growth was limited by phosphate deficiency at both temperatures (Table 1).

### Formation of aggregates

Total PV in roller tanks was initially similar in both temperature treatments, yielding  $43 \pm 8 \mu\text{l l}^{-1}$  at 8.5°C

Table 1. Concentration of inorganic nutrients and elemental stoichiometry of suspended particulate organic matter (POM) in the mesocosms at 8.5 and 2.5°C at the start of the aggregation experiment. Values are means  $\pm$  SD of duplicate mesocosms per temperature. POC: particulate organic carbon; PON: particulate organic nitrogen. nd: not detectable

|                                      | 8.5°C           | 2.5°C           |
|--------------------------------------|-----------------|-----------------|
| Inorganic nutrients                  |                 |                 |
| Nitrate ( $\mu\text{mol l}^{-1}$ )   | nd              | nd              |
| Phosphate ( $\mu\text{mol l}^{-1}$ ) | $0.07 \pm 0.02$ | $0.03 \pm 0.01$ |
| Stoichiometry of POM                 |                 |                 |
| [POC]:[PON]                          | $10.0 \pm 2.4$  | $16.6 \pm 2.1$  |
| [PON]:[POP]                          | $32.6 \pm 5.8$  | $29.5 \pm 0.2$  |

and  $33 \pm 4 \mu\text{l l}^{-1}$  at 2.5°C (Fig. 2). During the first 60 h of incubation, aggregates formed in roller tanks at both temperatures, reaching a maximum size of approximately 5 mm in diameter. Aggregates were comprised of diatom species mainly of the genera *Skeletonema* and *Chaetoceros*. After 60 h, the molar ratio of chl *a*:PON in aggregates was  $2.1 \pm 0.7$  at 8.5°C and 3.6

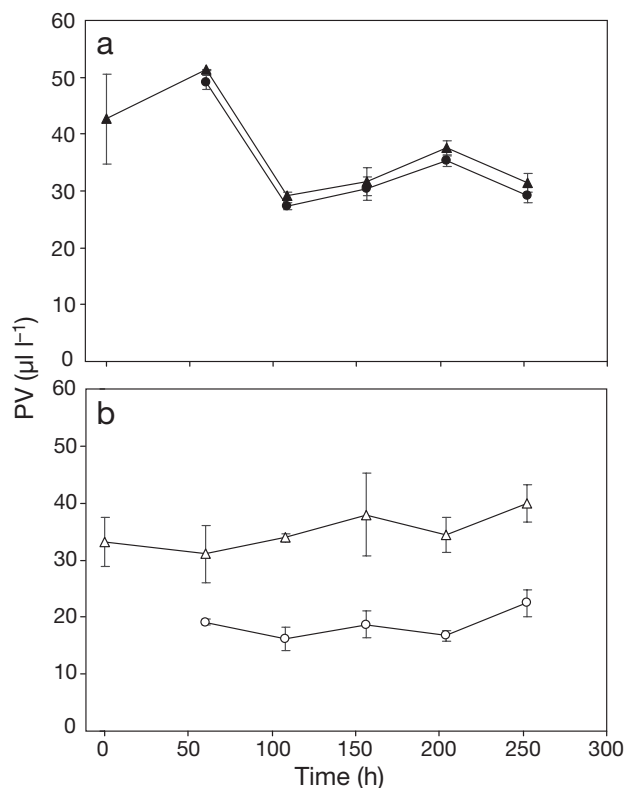


Fig. 2. Particle volume (PV) in aggregates and surrounding seawater (Total PV) and PV in aggregates (AGG) at (a) 2.5 and (b) 8.5°C. (▲): Total PV at 8.5°C; (●): PV in aggregates at 8.5°C; (Δ): total PV at 2.5°C; (○): PV in aggregates at 2.5°C. Values are means  $\pm$  SD of duplicate incubations per temperature

$\pm 1.3$  at 2.5°C. The proportions of total POM (AGG + SSW) included in aggregates were significantly higher at 8.5°C than at 2.5°C ( $p < 0.001$ ) during the whole experiment. Aggregates at 8.5°C contained between 93 and 96% of total PV, while aggregates at 2.5°C contained between 48 and 61% of total PV (Fig. 2). Between 81 and 96% of total POC, PON, and POP was contained in aggregates at 8.5°C, while aggregates at 2.5°C included between 43 and 69% (Table 2, Fig. 3). TEP concentration in aggregates and SSW at 8.5°C was significantly higher than at 2.5°C ( $p < 0.01$ ) (Fig. 4). At both temperatures, TEP concentration increased during dark incubation in the roller tanks. Concentration of total TEP started to increase after 156 h to values up to  $10.5 \pm 1.9$  mg Xeq l<sup>-1</sup> at 8.5°C and  $2.6 \pm 0.6$  mg Xeq l<sup>-1</sup> at 2.5°C. TEP concentration increased strongly in SSW, but only slightly in aggregates (Fig. 4). Ratios of TEP:PV were significantly higher in aggregates at 8.5°C than at 2.5°C ( $p < 0.001$ ). The mean ratio of TEP:PV over incubation time was  $117 \pm 41$   $\mu\text{g Xeq } \mu\text{l}^{-1}$  in aggregates at 8.5°C and  $37.0 \pm 19.1$   $\mu\text{g Xeq } \mu\text{l}^{-1}$  in aggregates at 2.5°C (Figs. 2 & 4). TEP in aggregates comprised a carbon amount of up to  $0.3 \pm 0.06$  mmol TEP-C l<sup>-1</sup> at 8.5°C and  $0.09 \pm 0.04$  mmol TEP-C l<sup>-1</sup> at 2.5°C.

### Microbial growth

The abundance of aggregate-associated bacteria after 60 h of incubation was  $1.8 \times 10^8 \pm 3.1 \times 10^7$  cells (ml AGG)<sup>-1</sup> at 8.5°C and  $2.0 \times 10^8 \pm 5.8 \times 10^7$  cells (ml AGG)<sup>-1</sup> at 2.5°C. At the same time point, the bacterial abundance in SSW was one order of magnitude lower, with  $1.9 \times 10^7 \pm 0.8 \times 10^7$  cells (ml SSW)<sup>-1</sup> at 8.5°C and  $0.8 \times 10^7 \pm 0.2 \times 10^7$  cells (ml SSW)<sup>-1</sup> at 2.5°C (Fig. 5). Bacteria showed exponential growth, with  $\mu = 0.007 \pm 0.001$  h<sup>-1</sup> in aggregates and  $\mu = 0.006 \pm 0.003$  h<sup>-1</sup> in SSW at 8.5°C. In contrast, at 2.5°C, bacter-

Table 2. Particulate organic nitrogen (PON) and particulate organic phosphorous (POP) in aggregates at the time of aggregate formation (60 h) and at the end of the experiment (252 h) ( $\mu\text{mol l}^{-1}$ , % of total), and loss from aggregates until the end of incubation (% loss). Values are means  $\pm$  SD of duplicate incubations at 8.5 and 2.5°C

|                        | 8.5°C        |               | 2.5°C       |               |
|------------------------|--------------|---------------|-------------|---------------|
|                        | PON          | POP           | PON         | POP           |
| 60 h                   |              |               |             |               |
| $\mu\text{mol l}^{-1}$ | $116 \pm 18$ | $3.9 \pm 1.0$ | $28 \pm 3$  | $1.0 \pm 0.0$ |
| % of total             | $91 \pm 2$   | $89 \pm 2$    | $59 \pm 12$ | $58 \pm 7$    |
| 252 h                  |              |               |             |               |
| $\mu\text{mol l}^{-1}$ | $110 \pm 16$ | $3.2 \pm 0.8$ | $38 \pm 11$ | $1.4 \pm 0.4$ |
| % of total             | $84 \pm 3$   | $78 \pm 0$    | $62 \pm 8$  | $60 \pm 3$    |
| % loss                 | $5 \pm 1$    | $17 \pm 1$    | –           | –             |

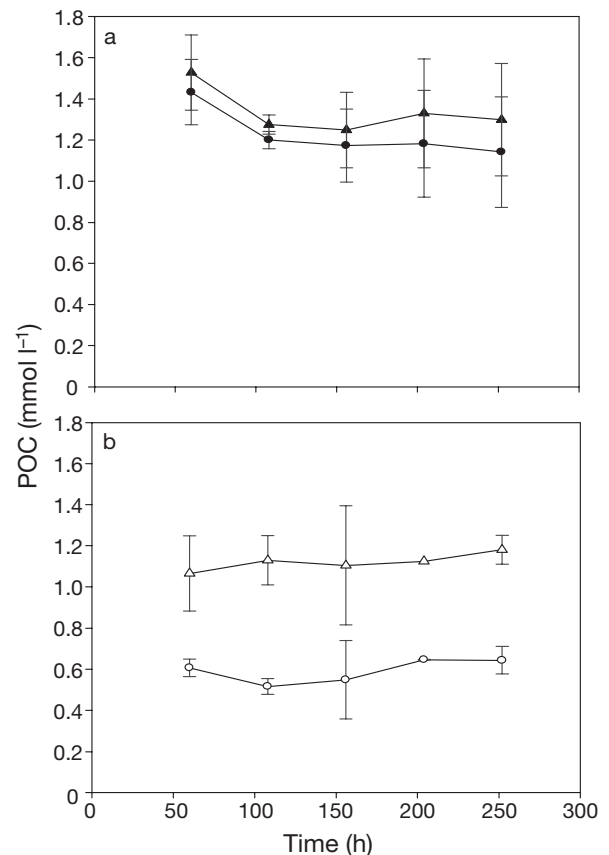


Fig. 3. Particulate organic carbon (POC) in aggregates and surrounding seawater (total POC) and POC in aggregates (AGG) at (a) 2.5 and (b) 8.5°C. ( $\blacktriangle$ ): Total POC at 8.5°C; ( $\bullet$ ): POC in aggregates at 8.5°C; ( $\triangle$ ): total POC at 2.5°C; ( $\circ$ ): POC in aggregates at 2.5°C. Values are means  $\pm$  SD of duplicate incubations per temperature

ial cell abundance in aggregates and SSW did not increase until the end of the incubation (Fig. 5).

Cumulatively calculated BBP in aggregates was  $0.72 \pm 0.06$   $\mu\text{mol C (ml AGG)}^{-1}$  and  $0.09 \pm 0.002$   $\mu\text{mol C (ml AGG)}^{-1}$  at 8.5 and 2.5°C, respectively. POC-specific BBP in aggregates at 8.5°C was about one order of magnitude higher than at 2.5°C ( $p < 0.01$ ) (Fig. 6).

### Activity of extracellular enzymes

In general, maximum hydrolysis rates ( $V_{\text{max}}$ ) of alkaline phosphatase and leucine-aminopeptidase were significantly higher than those of  $\alpha$ - and  $\beta$ -glucosidase in aggregates and SSW at both temperatures ( $p < 0.001$ ) (Tables 3 & 4). Temperature effects on  $V_{\text{max}}$  were observed for sugar- and protein-degrading extracellular

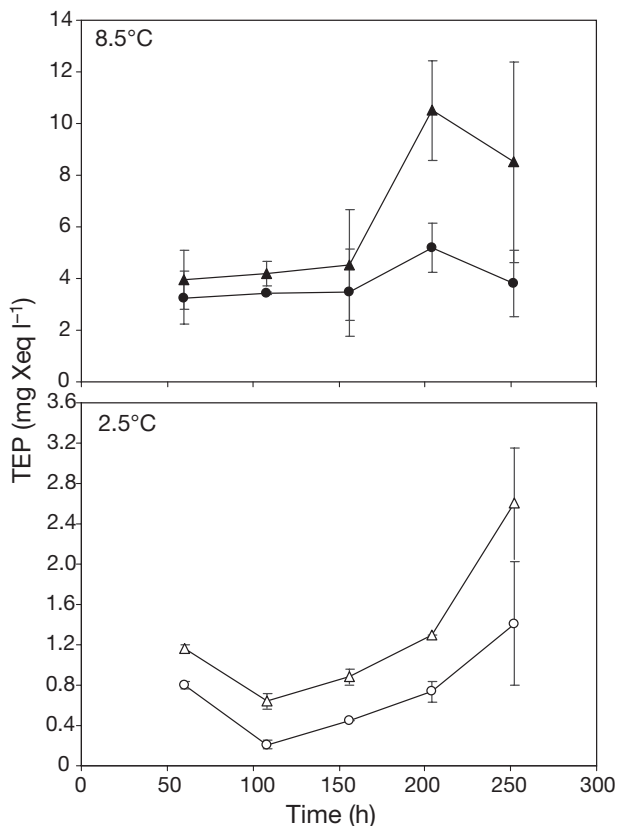


Fig. 4. Transparent exopolymer particles (TEP) in aggregates and surrounding seawater (total TEP) and proportion in aggregates (AGG) at 2.5 and 8.5°C. (▲): Total TEP at 8.5°C; (●): TEP in aggregates at 8.5°C; (Δ): total TEP at 2.5°C; (○): TEP in aggregates at 2.5°C. Values are means  $\pm$  SD of duplicate incubations per temperature

enzymes, where  $V_{\max}$  in aggregates and SSW was higher at 8.5 than at 2.5°C (Tables 3 & 4, Fig. 7). The differences between  $V_{\max}$  at 8.5 and at 2.5°C were significant for  $\beta$ -glucosidase and leucine-aminopeptidase in aggregates, and for  $\alpha$ -glucosidase,  $\beta$ -glucosidase, and leucine-aminopeptidase in SSW ( $p < 0.05$ ) (Tables 3 & 4). No significant effect on alkaline phosphatase was observed. The factor  $I_{V_{\max}}$  was calculated according to Eq. (7) in order to compare the different tested extracellular enzymes with regard to the temperature-induced enhancement of  $V_{\max}$ . A higher value of  $I_{V_{\max}}$  revealed that increased temperature had a stronger impact on  $V_{\max}$  of protein-degrading leucine-aminopeptidase than on  $V_{\max}$  of polysaccharide-degrading  $\alpha$ -glucosidase and  $\beta$ -glucosidase. The temporal development of  $V_{\max}$  in aggregates differed between the temperature treatments.  $V_{\max}$  of  $\beta$ -glucosidase, leucine-aminopeptidase, and alkaline phosphatase decreased over time in aggregates at 8.5°C, but increased in aggregates at 2.5°C (Fig. 7).

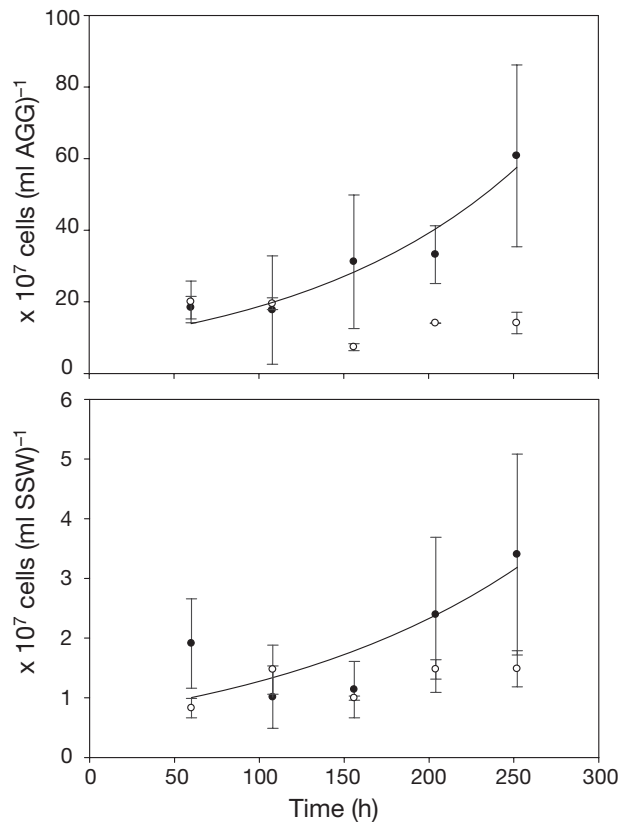


Fig. 5. Bacterial cell numbers in aggregates (AGG) and surrounding seawater (SSW) at 2.5 (○) and 8.5°C (●). Fitted curves show nonlinear regression with  $N_t = N_0 e^{\mu t}$ , where  $N_0$  is the initial cell number,  $\mu$  the growth rate constant, and  $t$  the time. Values are means  $\pm$  SD of duplicate incubations per temperature

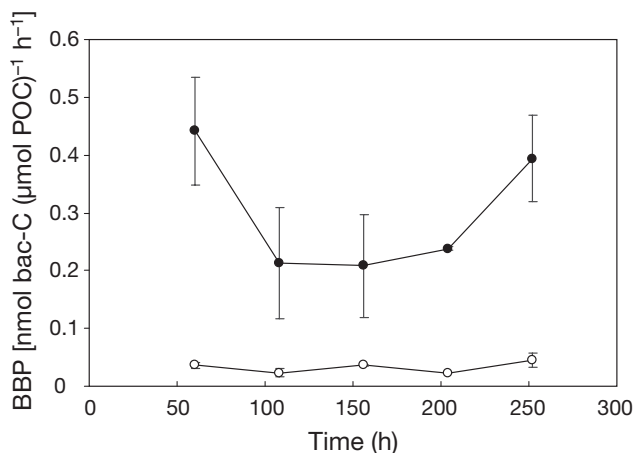


Fig. 6. Temporal development of bacterial biomass production (BBP) normalized to particulate organic carbon (POC) amounts in aggregates at 2.5 (○) and 8.5°C (●). Values are means  $\pm$  SD of duplicate incubations per temperature

Table 3. Activity of extracellular enzymes associated with aggregates. The enhancement factors  $I_{V_{\max}}$  and  $I_{V_{\max}/K_m}$  were calculated according to Eq. (7). Values are means  $\pm$  SD of duplicate incubations per temperature over time. \*Significant differences between temperature treatments ( $p < 0.05$ ). AGG: aggregates

| Enzyme                 | $V_{\max}$ [nmol (ml AGG) $^{-1}$ h $^{-1}$ ] |                | $I_{V_{\max}}$ | $V_{\max}/K_m$ (h $^{-1}$ ) |                 | $I_{V_{\max}/K_m}$ |
|------------------------|---|----------------|----------------|-----------------------------|-----------------|--------------------|
|                        | 8.5°C   | 2.5°C          |                | 8.5°C                       | 2.5°C           |                    |
| $\alpha$ -glucosidase  | 7.0 $\pm$ 1.5                                 | 4.5 $\pm$ 0.15 | 1.6            | 0.20 $\pm$ 0.02             | 0.05 $\pm$ 0.01 | 4.0*               |
| $\beta$ -glucosidase   | 21.0 $\pm$ 1.3                                | 5.0 $\pm$ 0.10 | 4.2*           | 0.65 $\pm$ 0.13             | 0.05 $\pm$ 0.01 | 13.0*              |
| Leucine-aminopeptidase | 386 $\pm$ 62                                  | 66.5 $\pm$ 4.0 | 5.8*           | 9.0 $\pm$ 1.0               | 3.0 $\pm$ 0.20  | 3.0*               |
| Alkaline phosphatase   | 221 $\pm$ 14                                  | 169 $\pm$ 37   | 1.3            | 108 $\pm$ 21.0              | 118 $\pm$ 0.20  | 0.9                |

Table 4. Activity of extracellular enzymes in the surrounding seawater (SSW). The enhancement factors  $I_{V_{\max}}$  and  $I_{V_{\max}/K_m}$  were calculated according to Eq. (7). Values are means over time  $\pm$  SD of duplicate incubations per temperature. \*Significant differences between temperature treatments ( $p < 0.05$ )

| Enzyme                 | $V_{\max}$ [nmol (ml AGG) $^{-1}$ h $^{-1}$ ] |                | $I_{V_{\max}}$ | $V_{\max}/K_m$ (h $^{-1}$ ) |                    | $I_{V_{\max}/K_m}$ |
|------------------------|---|----------------|----------------|-----------------------------|--------------------|--------------------|
|                        | 8.5°C   | 2.5°C          |                | 8.5°C                       | 2.5°C              |                    |
| $\alpha$ -glucosidase  | 180 $\pm$ 50                                  | 106 $\pm$ 14   | 1.6*           | 0.008 $\pm$ 0.0004          | 0.002 $\pm$ 0.0004 | 4.0*               |
| $\beta$ -glucosidase   | 320 $\pm$ 0.060                               | 171 $\pm$ 46   | 1.9*           | 0.006 $\pm$ 0.0025          | 0.002 $\pm$ 0.0017 | 3.0*               |
| Leucine-aminopeptidase | 7400 $\pm$ 2020                               | 1250 $\pm$ 149 | 5.9*           | 0.089 $\pm$ 0.020           | 0.040 $\pm$ 0.0010 | 2.2                |
| Alkaline phosphatase   | 2400 $\pm$ 1850                               | 1500 $\pm$ 127 | 1.6            | 1.58 $\pm$ 0.750            | 1.55 $\pm$ 0.34    | 1.0                |

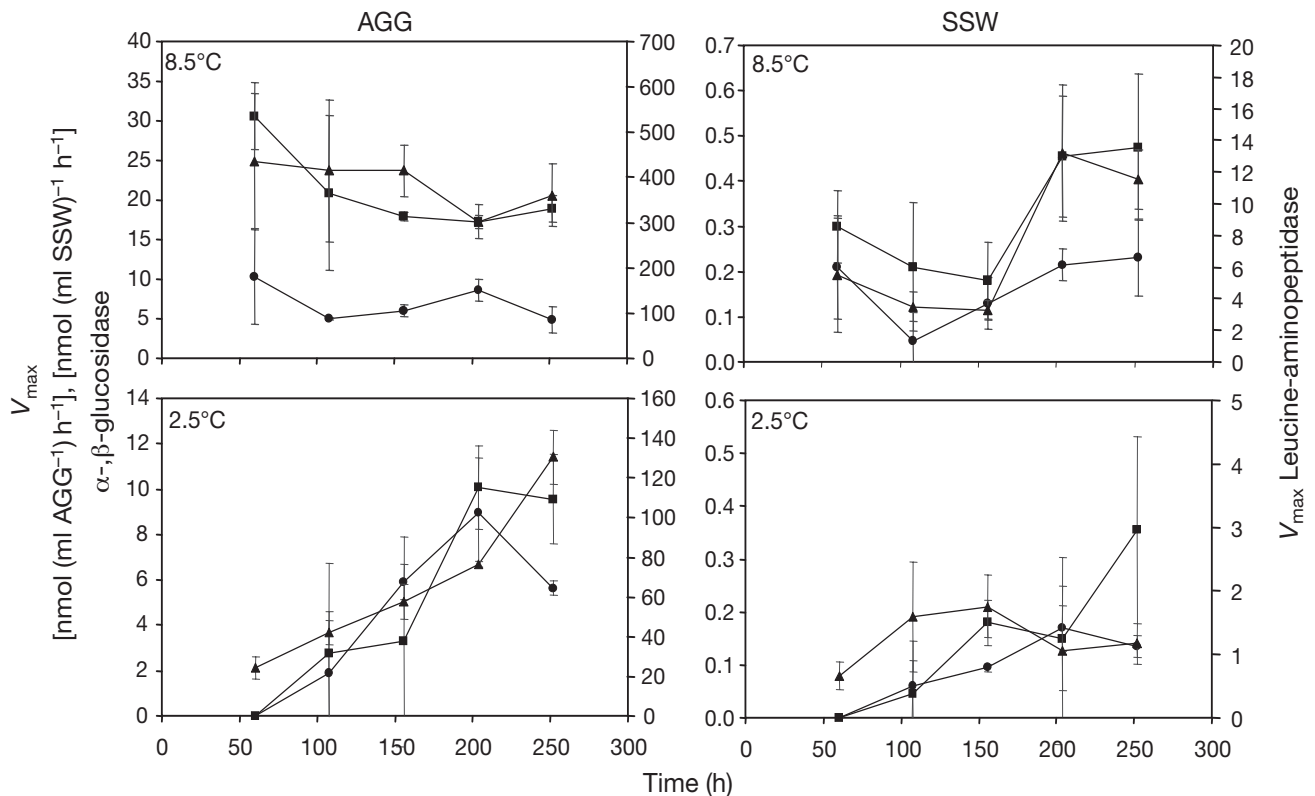


Fig. 7. Maximum hydrolysis rates ( $V_{\max}$ ) of extracellular enzymes in aggregates (AGG) and surrounding seawater (SSW) at 8.5 and 2.5°C. (●):  $\alpha$ -glucosidase; (■):  $\beta$ -glucosidase; (▲): leucine-aminopeptidase. Values are means  $\pm$  SD of duplicate incubations per temperature

A significantly higher ratio of  $V_{\max}/K_m$  indicated an enhanced activity of  $\alpha$ -glucosidase,  $\beta$ -glucosidase, and leucine-aminopeptidase at non-saturating substrate concentrations in aggregates and SSW at 8.5°C compared to 2.5°C ( $p < 0.05$ ) (Tables 3 & 4). This suggests an increased degradation efficiency of polysaccharides and proteins at higher temperature, even when substrate availability is low.  $I_{V_{\max}/K_m}$  was calculated according to Eq. (7) to compare the temperature effects on the efficiency of the different tested extracellular enzymes. As indicated by highest  $I_{V_{\max}/K_m}$  for  $\beta$ -glucosidase in aggregates, increased temperature had the strongest impact on the degradation efficiency of  $\beta$ -glycosidic-linked polysaccharides in aggregates (Tables 3 & 4).

The cell-specific  $V_{\max}$  of aggregate-associated bacteria was higher than those of bacteria in SSW for all tested extracellular enzymes and at both temperatures ( $p < 0.05$ ) (Table 5).  $I_{\text{cell-spec } V_{\max}}$  revealed that cell-specific  $V_{\max}$  of leucine-aminopeptidase in aggregates and SSW was significantly higher at 8.5 than at 2.5°C ( $p < 0.05$ ).

### Organic matter turnover in aggregates

Aggregates at 2.5°C did not show a net loss of PV and POM at the end of incubation time. In contrast, PV (Fig. 2) and POC (Fig. 3), as well as PON and POP (Table 2) decreased in aggregates at 8.5°C until the end of incubation. Aggregates at 8.5°C contained a PV of  $49.0 \pm 1.2 \mu\text{l l}^{-1}$  after 60 h of incubation. PV decreased to  $27.4 \pm 0.6 \mu\text{l l}^{-1}$  within the next 48 h, equivalent to a net loss of  $40 \pm 4\%$ . POC in aggregates at 8.5°C was  $1.4 \pm 0.2 \text{ mmol l}^{-1}$  after aggregate formation ( $t = 60$  h) and decreased by  $21 \pm 10\%$  until the end of incubation (Fig. 3). PON and POP in aggregates at 8.5°C were reduced by  $5 \pm 1\%$  and  $17 \pm 1\%$ , respectively, over the course of the incubation (Table 2).

The molar ratios of [POC]:[PON], [POC]:[POP], and [PON]:[POP] in aggregates at 8.5 and 2.5°C did not show a consistent trend over time. At both tempera-

tures, ratios were clearly higher than predicted by the Redfield ratio (Table 6). Ratios of [PON]:[POP] were not significantly different between the temperature treatments. In contrast, significantly lower ratios of [POC]:[PON] and [POC]:[POP] were obtained at 8.5 than at 2.5°C ( $p < 0.05$ ) due to higher amounts of PON and POP (Tables 1, 2 & 6). The initial concentration of dSi in SSW was below the detection limit at both temperatures. After 108 h of incubation at 8.5°C, dSi started to increase up to a final value of  $10.3 \pm 1.0 \mu\text{mol l}^{-1}$ . In contrast, dSi in SSW at 2.5°C did not increase significantly until the end of the incubation (Fig. 8).

### DISCUSSION

The experiment was set up to assess the effects of increased temperature on the formation, biogeochemical properties, and degradation of diatom aggregates. Two temperature treatments were applied during bloom development, aggregation of cells, and subsequent degradation of aggregates.

### Temperature effects on the formation and biogeochemical composition of aggregates

In the present study, higher temperature clearly increased the proportion of PV (Fig. 2) and POC (Fig. 3), as well as PON and POP contained in aggregates (Table 2). Thus, aggregates played a larger role

Table 6. Molar elemental ratios of particulate organic matter (POM) in aggregates at 8.5 and 2.5°C. Values are means  $\pm$  SD of duplicate incubations per temperature over time. POC: Particulate organic carbon; PON: particulate organic nitrogen; POP: particulate organic phosphorous

| Temperature | [POC]:[PON]    | [POC]:[POP]  | [PON]:[POP]    |
|-------------|----------------|--------------|----------------|
| 8.5°C       | $11.4 \pm 2.0$ | $349 \pm 56$ | $30.2 \pm 5.2$ |
| 2.5°C       | $20.2 \pm 2.1$ | $536 \pm 87$ | $26.8 \pm 4.8$ |

Table 5. Cell-specific potential hydrolysis rates ( $V_{\max}$ ) in aggregates (AGG) and surrounding seawater (SSW). The enhancement factor  $I_{\text{cell-spec } V_{\max}}$  was calculated according to Eq. (7). Values are means  $\pm$  SD of duplicate incubations per temperature over time. \*Significant differences between temperature treatments ( $p < 0.05$ )

| Enzyme                 | AGG $V_{\max}$ (amol cell <sup>-1</sup> h <sup>-1</sup> ) |                |                                  | SSW $V_{\max}$ (amol cell <sup>-1</sup> h <sup>-1</sup> ) |               |                                  |
|------------------------|---|----------------|----------------------------------|---|---------------|----------------------------------|
|                        | 8.5°C   | 2.5°C          | $I_{\text{cell-spec } V_{\max}}$ | 8.5°C   | 2.5°C         | $I_{\text{cell-spec } V_{\max}}$ |
| $\alpha$ -glucosidase  | $33 \pm 21$   | $57 \pm 15$    | 0.6                              | $9 \pm 1$   | $10 \pm 1$    | 0.9                              |
| $\beta$ -glucosidase   | $95 \pm 29$   | $61 \pm 30$    | 1.6                              | $19 \pm 8$  | $15 \pm 3$    | 1.3                              |
| Leucine-aminopeptidase | $1717 \pm 532$  | $521 \pm 23$   | 3.3*                             | $387 \pm 96$  | $101 \pm 342$ | 3.8*                             |
| Alkaline phosphatase   | $1081 \pm 672$  | $1220 \pm 516$ | 0.89                             | $131 \pm 69$  | $125 \pm 42$  | 1.0                              |

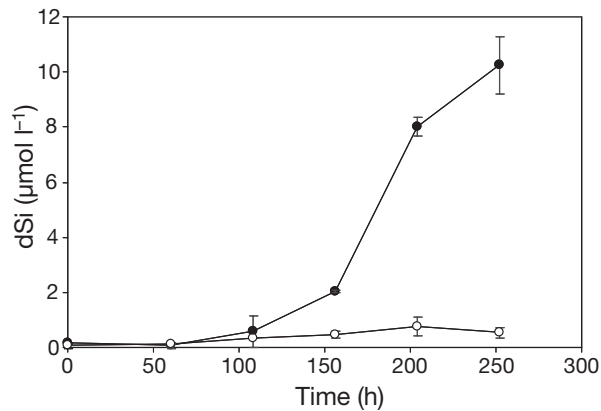


Fig. 8. Development of dissolved silicate concentration (dSi) in surrounding seawater (SSW) during incubation at 2.5°C (○) and 8.5°C (●). Values are means  $\pm$  SD of duplicate incubations per temperature

in the overall turnover of organic matter at elevated temperature. In the ocean, larger proportions of POC, PON, and POP in aggregates represent a more efficient allocation of organic matter for potential export via fast particle sinking.

Because we did not investigate the aggregation process directly, we can only speculate about the potential mechanisms that were responsible for enhanced aggregate formation at higher temperature. The initial PV at elevated and *in situ* temperatures was not significantly different; therefore, similar collision rates between particles can be assumed for both treatments. Instead, higher TEP:PV ratios likely enhanced aggregation at the elevated temperature (Figs. 2 & 4), since TEP have been identified to promote aggregation by increasing the stickiness of particles (Alldredge et al. 1993, Passow et al. 1994, Engel 2000).

#### Transparent exopolymer particles (TEP)

TEP contain primarily polysaccharides, and are therefore carbon-rich and poor in nitrogen. The formation of TEP from dissolved sugars is an important process in the conversion of dissolved organic carbon into POC (Engel et al. 2004). The organic matter used in the present study contained high amounts of TEP (Fig. 4), which was related to exudation by diatoms suffering from nutrient depletion in the mesocosms (J. Wohlers et al. unpubl. data). A further increase in TEP concentration was observed during dark incubation: TEP concentration was significantly higher at elevated temperature than at *in situ* temperature (Fig. 4). It seems likely that the high abundance of bacteria had a substantial effect on the formation of TEP by modifying precursors originating from phytoplankton exudation. Bacterial degradation activity increases the proportion

of deoxy sugars in extracellular polysaccharides (EPS), enhancing the hydrophobic feature of EPS and the formation of TEP (Girollo et al. 2003). Bacteria also produce considerable amounts of exopolymers, in particular when attached to surfaces (Decho 1990). The formation of an exopolymer capsule enables marine bacteria to attach to surfaces (Heissenberger et al. 1996). TEP can be generated by releasing polysaccharide fibrils from the capsular material. However, this process was of minor importance in our experiment. Cell-specific TEP production of 0.1 fg Xeq cell<sup>-1</sup> h<sup>-1</sup> was determined for coastal North Sea bacterioplankton (Stoderegger & Herndl 1999). Assuming this rate, only 0.8 and 3.6% of TEP production in aggregates at *in situ* and elevated temperatures, respectively, could be related to bacterial production.

#### Temperature sensitivity of bacterial growth and degradation activity

Aggregates harbour diverse and large bacterial communities, since they provide a beneficial substrate for bacterial growth. In accordance with previous studies (Alldredge et al. 1986, Herndl 1988, Karner & Herndl 1992, Ploug & Grossart 2000, Grossart et al. 2003), we observed an enrichment of bacteria in aggregates (Fig. 5), as well as increased cell-specific enzymatic rates of aggregate-associated bacteria (Table 5). It has been suggested that the acceleration of metabolic rates after attachment allows bacteria to maximize benefit from substrate-replete aggregate surfaces (Grossart et al. 2007).

In the present study, elevated temperature substantially increased rates of bacterial growth and degradation activity on aggregates as well as in the SSW (Tables 3 to 5, Figs. 5 to 7). Temperature effects on bacterial extracellular enzymes were strong enough to increase the loss of POM from aggregates, accelerating the turnover of aggregates at elevated temperature (Table 2, Figs. 2 & 3). Extracellular enzymes are produced by bacteria to hydrolyze polymers into subunits, which can then be taken up by the cell. Their hydrolytic activity drives the solubilization of particles and is therefore crucial for the degradation of aggregates (Smith et al. 1992). Temperature effects on extracellular enzymes integrated 2 aspects: (1) rising temperature enhanced the enzymatic degradation of organic matter thermodynamically by an increase of the rate constants  $k_1$  and  $k_2$  given in Eq. (3); and (2) aggregates at elevated temperature showed higher abundances of bacteria and, therefore, higher production of extracellular enzymes (Fig. 5). Starting with similar bacterial abundances at both temperatures, only aggregates and SSW at elevated temperature pro-

vided conditions beneficial for bacterial growth (Figs. 5 & 6). Thus, higher enzymatic activities in aggregates at elevated temperature were supported by an increased enzyme production of a larger bacterial community.

Cell-specific rates of extracellular enzyme activity (cell-specific  $V_{\max}$ ) allow for a differentiation between these 2 aspects, since they exclude effects due to temperature-related differences in bacterial abundance. Significant differences in cell-specific  $V_{\max}$  of leucine-aminopeptidase between the 2 temperatures indicated that temperature effects on the catalytic step of the enzymatic reaction were decisive for the increased rate of enzymatic protein hydrolysis. In contrast, cell-specific  $V_{\max}$  of  $\alpha$ -glucosidase and  $\beta$ -glucosidase did not reveal significant differences between the 2 treatments, suggesting the increased enzymatic degradation of polysaccharides at elevated temperature was primarily promoted by a larger bacterial community.

Tested extracellular enzymes revealed different sensitivities to elevated temperature, leading to differences in activity ratios of polysaccharide-, protein-, and organic phosphate-degrading enzymes between the 2 temperatures (Tables 3, 4 & 5). However, we did not determine an effect of different activity ratios on the stoichiometry of POM. Nevertheless, different temperature sensitivities of extracellular enzymes may have changed the biochemical composition of labile organic matter in aggregates and SSW, which is highly relevant for bacterial growth, but accounts only for a minor proportion of total organic matter. Different control mechanisms of enzyme expression further complicate the projection of degradation rates of bulk organic carbon, nitrogen, and phosphate from the magnitude of enzymatic activity. Extracellular glucosidase activity is repressed by high concentrations of the monomeric end-products and, therefore, is regulated by ambient substrate concentrations (Chróst 1991). In contrast, leucine-aminopeptidase was shown to be repressed only by specific amino acids known to be rare in seawater, e.g. histidine and phenylalanine. High protease activity at low concentrations of labile substrates was found in a previous study (Christian & Karl 1998). It is assumed that a constitutively high leucine-aminopeptidase activity ensures an efficient supply with nitrogenous substrates, which are often limiting bacterial growth (Christian & Karl 1998).

The activity of extracellular enzymes in aggregates showed different temporal trends at the 2 temperatures. Continuously increasing enzymatic rates in aggregates at *in situ* temperature suggest a sufficient substrate supply to bacteria until the end of incubation, supporting the assumption that aggregate degradation was temporally impeded due to lower temperature and not substrate limitation. Enzymatic rates in aggregates at elevated temperature decreased with time, coincid-

ing with an exponential increase in cell numbers (Figs. 5 & 7). A similar coincidence of increasing bacterial cell density and decreasing metabolic rates in aggregates was observed for glucose and leucine uptake (Azúa et al. 2007). Decreasing uptake rates were suggested to indicate a quantitative and qualitative impoverishment of organic matter in aggregates with time, an explanation that also seems reasonable for temporally decreasing enzymatic activity in aggregates at elevated temperature.

### Degradation of particulate matter in aggregates

The flux of organic matter in aggregates and the related particle concentration both decrease continuously with depth (Martin et al. 1987, Kiørboe 2001). In the present study, aggregates at elevated temperature showed a net loss of PV, POC, PON, and POP during the incubation, while no net loss of PV and POM was determined from aggregates at *in situ* temperature (Table 2, Figs. 2 & 3). The total duration of the experiment was restricted to 11 d, and 8 d remained after the formation of aggregates. Thus, our experimental results reflect an early phase of degradation, and elevated temperature clearly enhanced the remineralization of aggregates during this early phase. As no net loss occurred from aggregates at *in situ* temperature, acceleration of remineralization cannot be expressed in terms of a temperature-normalized factor. It must be assumed that degradation of aggregated POM at *in situ* temperature occurs on longer time scales. Hence, our results indicate a temporal lag of at least 8 d between aggregate formation and degradation at *in situ* temperature, but an immediate onset of aggregate degradation at elevated temperature. This finding is in good accordance with results from the AQUASHIFT mesocosm study 2005, where a diminished temporal lag between the peaks of primary production and bacterial production also suggested an earlier start of organic matter degradation at elevated temperature (Hoppe et al. 2008). Considering that degradation of aggregates in the ocean coincides with sinking, a significantly earlier onset of aggregate degradation at elevated temperature would lead to an enhanced remineralization of aggregated POM especially in the upper ocean.

Aggregates at elevated temperature showed a discrepancy between the net loss of POM and the net loss of PV. PV was reduced more strongly than POM by the end of the incubation, and revealed a much lower variability between replicates (Figs. 2 & 3). It should be noted that particles not detectable by the Coulter counter, e.g. hydrated gels and particles smaller than 2.7  $\mu\text{m}$ , contributed significantly to the pool of POM.

TEP are not quantified by the Coulter counter, but also contain organic carbon. Aggregates at elevated temperature included TEP of up to 5.2 mg Xeq l<sup>-1</sup> (Fig. 4). TEP can be considered as an integral part of aggregates due to its function as glue. It was therefore estimated that up to 0.3 mmol TEP-C l<sup>-1</sup> were included in aggregates at elevated temperature. Thus, the carbon loss from aggregates at elevated temperature (Fig. 3) was partially compensated by production of TEP-C (Fig. 4).

Concentration ratios of [POC]:[PON], [POC]:[POP], and [PON]:[POP] in aggregates did not reveal consistent temporal trends at both temperatures. The ratios of [POC]:[PON] and [POC]:[POP] were significantly lower in aggregates at elevated temperature due to stoichiometric differences in the sedimented organic matter collected from the mesocosms (Tables 1, 2 & 6). A positive relationship between degradation rates and nitrogen and phosphate content of organic matter was found when data across a broad spectrum of detritus, from unicellular algae to terrestrial macrophytes, were included in the statistical analysis. Conversely, this general relationship was not confirmed for the degradation of several distinct types of detritus, including debris derived from phytoplankton (Enríquez et al. 1993 and references therein). It seems unlikely that the lack of aggregate remineralization at *in situ* temperature was due to an unsuitable stoichiometry and quality of POM in our experiment. Initial chl *a*:PON ratios of aggregates at the 2 temperatures indicated similar freshness of algal cells. We therefore assume that sufficient amounts of labile organic matter were available for bacteria at both temperatures. Hence, increased temperature can be regarded as the leading factor for an accelerated degradation at higher temperature in this short-term incubation. However, potential effects of POM stoichiometry on the degradation of aggregates on time scales exceeding the incubation period of our experiment cannot be excluded.

Decomposition of diatom cells is tightly coupled to the dissolution of silica from diatom frustules (Ragueneau et al. 2006). Concentration of dSi in the SSW at elevated temperature increased by 10 μmol l<sup>-1</sup> during the last 6 d of incubation (Fig. 8). This increasing concentration indicated dissolution of biogenic silica (bSi). In contrast, no increase was determined at *in situ* temperature, indicating that no dissolution of bSi occurred (Fig. 8). Dissolution of bSi can start after microbial degradation of the organic layer associated with the diatom surface (Bidle & Azam 2001). It can therefore be assumed that the lower bacterial abundance (Fig. 5) and lower protease activity (Tables 3 & 4, Fig. 7) at *in situ* temperature were not sufficient to remove the protecting outer organic layer associated with diatom frustules. The incubated natural diatom community con-

sisted mainly of *Chaetoceros* spp. and *Skeletonema* spp., for which a Si:C ratio of about 0.1 can be assumed (Brzezinski 1985). Assuming that all POC was derived from diatoms, a concentration of approximately 14 μmol bSi l<sup>-1</sup> can be estimated for the SSW at elevated temperature. Hence, dissolution of bSi from diatoms dispersed in the SSW could quantitatively explain the increase in concentration. However, following the linear initial rate approach (Greenwood et al. 2001), a bSi dissolution rate of 0.12 d<sup>-1</sup> was obtained for POM at 8.5°C. This rate is 3 times higher than previously found in studies that were conducted at temperatures 5 or 10°C higher than the present study (Bidle & Azam 2001, Moriceau et al. 2007). Therefore, it seems likely that the increasing dSi concentration in the SSW at elevated temperature was substantially influenced by bSi dissolution from aggregates. Aggregates leak solutes containing high concentration of dissolved compounds (Smith et al. 1992, Kiørboe 2001), and previous studies have revealed an acceleration of silica dissolution from dispersed diatoms with increasing temperature (Lewin 1961, Kamatani 1982). Results of the present study indicate a temperature-induced acceleration of bSi dissolution from diatom aggregates.

#### Extrapolation of experimental results to a larger scale — implications for the future ocean

Extrapolating the results of the present study to natural systems bears considerable uncertainties. Nevertheless, manipulative laboratory experiments are a valuable tool to assess potential consequences of global change, such as ocean warming and acidification, for natural systems. Formation of large particle aggregates and the rates of their decomposition by heterotrophic bacteria are important processes that determine the efficiency of particle export in the ocean (Fowler & Knauer 1986, Kiørboe et al. 1996, Smith et al. 1992). Our experimental results indicate that elevated temperature increases both the probability of aggregate formation and the rate of bacterial degradation of aggregated organic matter. Effects of elevated temperature on export efficiencies in the future ocean will likely depend on the relative magnitude of increased aggregation versus enhanced bacterial degradation. It is important to consider that aggregation and degradation processes in the ocean are often vertically separated. While the high particle abundances required for the aggregation of POM are mostly achieved in the surface layer, bacterial degradation of sinking aggregates continues in the subsurface strata. In shallow coastal areas like the Kiel Fjord, where temperatures are homogeneous from surface to bottom, climate warming will most probably affect the entire water col-

umn. Here, temperature-enhanced organic matter degradation and the resulting acceleration of organic carbon turnover are likely to be the dominant effects of warming. In deep water bodies, the temperature increase at the surface may be disproportionately high compared to subsurface strata. Here, the enhancement of aggregate formation may predominate and increase the export of carbon, since sinking of aggregates to cooler depths may mitigate the effects of ocean warming on bacterial degradation. Other factors, such as phytoplankton growth, light, and nutrient availability, will further affect the timing of formation and bacterial colonization of aggregates and, consequently, co-determine the export efficiencies of aggregates. Therefore, we suppose that *in situ* effects of warming on the formation and degradation of phytoplankton aggregates in the ocean are of higher complexity, depending on the depth penetration of increasing ocean temperature as well as the timing of biological processes.

**Acknowledgements.** This study was supported by the Helmholtz Association (HZ-NG-102) and the German Research Foundation (DFG) (priority program 1162 AQUASHIFT, Project No. RI 598/2-1). We thank P. Breithaupt, R. Koppe, K. Walther, H. Mempel, H. Johannsen, M. Schartau, and P. Fritsche for help in sample processing, and H. Ploug for fruitful comments. Two anonymous referees are acknowledged for their suggestions on improving this publication.

#### LITERATURE CITED

- Allredge AL, Silver ML (1988) Characteristics, dynamics and significance of marine snow. *Prog Oceanogr* 20:41–82
- Allredge AL, Cole JJ, Caron DA (1986) Production of heterotrophic bacteria inhabiting macroscopic aggregates (marine snow) from surface waters. *Limnol Oceanogr* 31:68–78
- Allredge AL, Passow U, Logan BE (1993) The abundance and significance of a class of large transparent organic particles in the ocean. *Deep-Sea Res I* 40:1131–1140
- Arnosti C (2004) Speed bumps and barricades in the carbon cycle: substrate structural effects on carbon cycling. *Mar Chem* 92:263–273
- Asper VL (1987) Measuring the flux and sinking speed of marine snow aggregates. *Deep-Sea Res A* 34:1–17
- Azúa I, Unanue M, Ayo B, Artolozaga I, Iriberrí J (2007) Influence of age of aggregates and prokaryotic abundance on glucose and leucine uptake by heterotrophic marine prokaryotes. *Int Microbiol* 10:13–18
- Bidle KD, Azam F (2001) Bacterial control of silicon regeneration from diatom detritus: Significance of bacterial ecto-hydrolases and species identity. *Limnol Oceanogr* 46:1606–1623
- Brock TD (1981) Calculating solar radiation for ecological studies. *Ecol Model* 14:1–19
- Brzezinski MA (1985) The Si:C:N ratio of marine diatoms: interspecific variability and the effect of some environmental variables. *J Phycol* 21:347–357
- Christian JR, Karl DM (1998) Ectoaminopeptidase specificity and regulation in antarctic marine pelagic microbial communities. *Aquat Microb Ecol* 15:303–310
- Chróst RJ (1991) Environmental control of the synthesis and activity of aquatic microbial ectoenzymes. In: Chróst RJ (ed) *Microbial enzymes in aquatic environments*. Springer, New York, p 29–59
- Decho AW (1990) Microbial exopolymer secretion in the ocean environments: their role(s) in food webs and marine processes. *Oceanogr Mar Biol Annu Rev* 28:73–153
- Ducklow HW, Carlson CA (1992) Oceanic bacterial production. *Adv Microb Ecol* 12:113–181
- Engel A (2000) The role of transparent exopolymer particles (TEP) in the increase in apparent particle stickiness (alpha) during the decline of a diatom bloom. *J Plankton Res* 22:485–497
- Engel A, Passow U (2001) Carbon and nitrogen content of transparent exopolymer particles (TEP) in relation to their Alcian Blue adsorption. *Mar Ecol Prog Ser* 219:1–10
- Engel A, Meyerhöfer M, von Bröckel K (2002) Chemical and biological composition of suspended particles and aggregates in the Baltic Sea in summer (1999). *Estuar Coast Shelf Sci* 55:729–741
- Engel A, Thoms S, Riebesell U, Rochelle-Newall E, Zonder-van I (2004) Polysaccharide aggregation as a potential sink of marine dissolved organic carbon. *Nature* 428:929–932
- Enriquez S, Duarte CM, Sand-Jensen K (1993) Patterns in decomposition rates among photosynthetic organisms: the importance of detritus C:N:P content. *Oecologia* 94:457–471
- Fowler SW, Knauer GA (1986) Role of large particles in the transport of elements and organic compounds through the oceanic water column. *Prog Oceanogr* 16:147–194
- Fuhrman JA, Azam F (1982) Thymidine incorporation as a measure of heterotrophic bacterioplankton production in marine surface waters: evaluation and field results. *Mar Biol* 66:109–120
- Giroldo D, Vieira AAH, Smestad Paulsen B (2003) Relative increase of deoxy sugars during microbial degradation of an extracellular polysaccharide released by a tropical freshwater *Thalassiosira* sp. (Bacillariophyceae). *J Phycol* 39:1109–1115
- Greenwood JE, Truesdale VW, Rendell AR (2001) Biogenic silica dissolution in seawater—in vitro chemical kinetics. *Prog Oceanogr* 48:1–23
- Grossart HP, Ploug H (2001) Microbial degradation of organic carbon and nitrogen in diatom aggregates. *Limnol Oceanogr* 46:267–277
- Grossart HP, Hietanen S, Ploug H (2003) Microbial dynamics on diatom aggregates in Øresund, Denmark. *Mar Ecol Prog Ser* 249:69–78
- Grossart HP, Tang KW, Kiørboe T, Ploug H (2007) Comparison of cell-specific activity between free-living and attached bacteria using isolates and natural assemblages. *FEMS Microbiol Lett* 266:194–200
- Heissenberger A, Leppard GG, Herndl GJ (1996) Ultrastructure of marine snow. II. Microbiological considerations. *Mar Ecol Prog Ser* 135:299–308
- Herndl GJ (1988) Ecology of amorphous aggregations (marine snow) in the Northern Adriatic Sea: II. Microbial density and activity in marine snow and its implication to overall pelagic processes. *Mar Ecol Prog Ser* 48:265–275
- Hoppe HG (1983) Significance of exoenzymatic activities in the ecology of brackish water: measurements by means of methylumbelliferyl-substrates. *Mar Ecol Prog Ser* 11:299–308

- Hoppe HG, Ducklow H, Karrasch B (1993) Evidence for dependency of bacterial growth on enzymatic hydrolysis of particulate organic matter in the mesopelagic ocean. *Mar Ecol Prog Ser* 93:277–283
- Hoppe HG, Breithaupt P, Walther K, Koppe R, Bleck S, Sommer U, Jürgens K (2008) Climate warming during winter affects the coupling between phytoplankton and bacteria during the spring bloom: results from a mesocosm study. *Aquat Microb Ecol* 51:105–115
- Intergovernmental Panel on Climate Change (IPCC) (2001) Contribution of Working Group II to the third assessment report of the Intergovernmental Panel on Climate Change. In: McCarthy JJ, Canziani OF, Leary NA, Dokken DJ, White KS (eds) *Climate change 2001: impacts, adaptations and vulnerability*. Cambridge University Press, Cambridge
- Jiménez-Mercado A, Cajal-Medrano R, Maske H (2007) Marine heterotrophic bacteria in continuous culture, the bacterial carbon growth efficiency, and mineralization of excess substrate and different temperature. *Microb Ecol* 54:56–64
- Kamatani A (1982) Dissolution rates of silica from diatoms decomposing at various temperatures. *Mar Biol* 68:91–96
- Karner M, Herndl GJ (1992) Extracellular enzymatic activity and secondary production in free-living and marine snow associated bacteria. *Mar Biol* 113:341–347
- Kjørboe T (2001) Formation and fate of marine snow: small-scale processes with large-scale implications. *Sci Mar* 65:57–71
- Kjørboe T, Hansen JLS, Alldredge AL, Jackson GA, and others (1996) Sedimentation of phytoplankton during a diatom bloom: rates and mechanisms. *J Mar Res* 54: 1123–1148
- Koroleff F (1977) The international intercalibration exercises for nutrient methods. ICES Cooperative Research Report no. 67, ICES, Charlottenlund
- Lewin J (1961) The dissolution of silica from diatom walls. *Geochim Cosmochim Acta* 21:182–198
- Martin JH, Knauer GA, Karl DM, Broenkow WW (1987) VERTEX: carbon cycling in the northeast Pacific. *Deep-Sea Res A* 34:267–285
- Moriceau B, Garvey M, Ragueneau O, Passow U (2007) Evidence for reduced biogenic silica dissolution rates in diatom aggregates. *Mar Ecol Prog Ser* 333:129–142
- Passow U, Alldredge AL (1995) A dye-binding assay for the spectrophotometric measurement of transparent exopolymer particles (TEP). *Limnol Oceanogr* 40:1326–1335
- Passow U, Alldredge AL, Logan BE (1994) The role of particulate carbohydrate exudates in the flocculation of diatom blooms. *Deep-Sea Res I* 41:335–357
- Ploug H, Grossart HP (2000) Bacterial growth and grazing on diatom aggregates: respiratory carbon turnover as a function of aggregate size and sinking velocity. *Limnol Oceanogr* 45:1467–1475
- Pomeroy L, Wiebe WJ (2001) Temperature and substrates as interactive limiting factors for marine heterotrophic bacteria. *Aquat Microb Ecol* 23:187–204
- Porter KG, Feig YS (1980) The use of DAPI for identifying and counting microflora. *Limnol Oceanogr* 25:943–947
- Ragueneau O, Schultes S, Bidle K, Claquin P, Moriceau B (2006) Si and C interactions in the world ocean: importance of ecological processes and implications for the role of diatoms in the biological pump. *Global Biogeochem Cycles* 20:GB4S02
- Rath J, Herndl GJ (1994) Characteristics and diversity of  $\beta$ -D-glucosidase (EC 3.2.1.21) activity in marine snow. *Appl Environ Microbiol* 60:807–813
- Redfield AC, Ketchum BM, Richards FA (1963) The influence of organisms on the composition of seawater. In: Hill MN (ed) *The sea*. Wiley, New York, p 26–77
- Riebesell U (1991) Particle aggregation during a diatom bloom. II. Biological aspects. *Mar Ecol Prog Ser* 69: 281–291
- Simon M (2002) Microbial ecology of organic aggregates in aquatic ecosystems. *Aquat Microb Ecol* 28:175–211
- Smetacek V (1985) Role of sinking in diatom life history cycles: ecological, evolutionary and geological significance. *Mar Biol* 84:239–251
- Smith DC, Simon M, Alldredge AL, Azam F (1992) Intense hydrolytic enzyme activity on marine aggregates and implications for rapid particle dissolution. *Nature* 359: 139–142
- Sommer U, Aberle N, Engel A, Hansen T and others (2007) An indoor mesocosm system to study the effect of climate change on late winter and spring succession of Baltic Sea phyto- and zooplankton. *Oecologia* 150:655–667
- Stoderegger KE, Herndl GJ (1999) Production of exopolymer particles by marine bacterioplankton under contrasting turbulence conditions. *Mar Ecol Prog Ser* 189:9–16
- Strickland JDH, Parsons TR (1974) *A practical handbook of seawater analysis*. Fisheries Research Board of Canada, Bulletin 167, Ottawa
- Thornton DCO, Thake B (1998) Effect of temperature on the aggregation of *Skeletonema costatum* (Bacillariophyceae) and the implication for carbon flux in coastal waters. *Mar Ecol Prog Ser* 174:223–231
- Wiebe WJ, Sheldon WM Jr, Pomeroy LR (1992) Bacterial growth in the cold: evidence for an enhanced substrate requirement. *Appl Environ Microbiol* 58:359–364

*Editorial responsibility: Patricia Glibert, Cambridge, Massachusetts, USA*

*Submitted: June 25, 2008; Accepted: December 5, 2008  
Proofs received from author(s): February 26, 2009*